

# A Facile Approach To Remediate the Microenvironment of Saline–Alkali Soil

Na Jiang,<sup>†,‡</sup> Dongqing Cai,<sup>‡,§</sup> Lulu He,<sup>†,‡</sup> Naiqin Zhong,<sup>||</sup> Han Wen,<sup>\*,†</sup> Xin Zhang,<sup>\*,†</sup> and Zhengyan Wu<sup>\*,‡,§</sup>

<sup>†</sup>School of Life Sciences, Anhui Agricultural University, 130 West Changjiang Road, Hefei 230036, People's Republic of China

<sup>‡</sup>Key Laboratory of Ion Beam Bioengineering, Hefei Institutes of Physical Science, Chinese Academy of Sciences and Anhui Province, 350 Shushanhu Road, Hefei, Anhui 230031, People's Republic of China

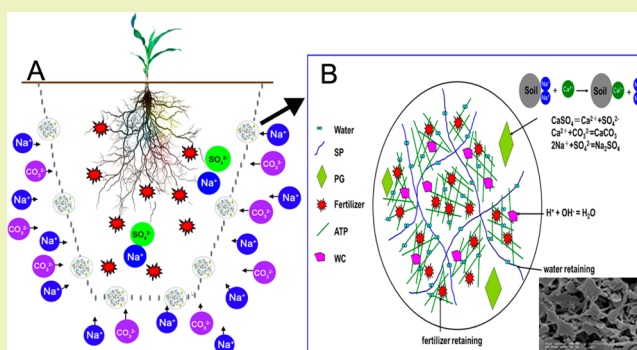
<sup>§</sup>Bioenergy Forest Research Center of State Forestry Administration, 350 Shushanhu Road, Hefei 230031, People's Republic of China

<sup>||</sup>Institute of Microbiology, Chinese Academy of Sciences, No. 1 Beichen West Road, Beijing 100101, People's Republic of China

## S Supporting Information

**ABSTRACT:** A facile approach to remediate the microenvironment of saline–alkali soil (SS) was developed using a novel fertilizer named saline–alkali soil remediating fertilizer (SSRF). SSRF was obtained by adding a nanocomposite as the saline–alkali soil remediating agent (SSRA) made up of attapulgite (ATP), phosphogypsum (PG), sodium polyacrylate (SP), and weathered coal (WC) to a traditional fertilizer (TF). SSRF could form micro/nanonetworks in SS and display a high retaining capacity on water and fertilizer nutrients because of the hydrogen bonds between SSRA and water molecules, urea, or  $\text{NH}_4\text{Cl}$ . In addition, SSRF could effectively reduce the salinity and alkalinity in SS through ion exchange, deactivation, and pH adjusting. Thus, SSRF could significantly improve the microenvironment of SS, which could facilitate the growth of crops and increase the saline–alkaline tolerance of crops.

**KEYWORDS:** Saline–alkali soil, Microenvironment, Retaining, Remediate, Attapulgite



## INTRODUCTION

At present, the salinization and alkalization of soil are widespread and severe environmental problems threatening the sustainability of our lands.<sup>1</sup> According to the incomplete statistics from the United Nations Educational, Scientific and Cultural Organization (UNESCO) and the Food and Agriculture Organization (FAO) of the United Nations, over 100 countries possess different types of saline–alkali soil (SS). The entire SS area is about 9.5438 billion  $\text{hm}^2$ , which accounts for 10% of the arable land in the world.

Internationally, for over 100 years, many efforts have been made to control and exploit saline–alkali land. As early as 150 years ago, Russia began to build farmland shelterbelts to prevent the salinization and alkalization of soil. Thereafter, many countries, such as Pakistan, India, Egypt, Israel, and Australia, have done a lot of research in terms of governance on saline–alkali land.<sup>2,3</sup> Currently, the methods of remediating SS mainly include physical (water conservation), biological (phytoremediation),<sup>4,5</sup> and chemical (desulfurization gypsum, furfural slag, vermicompost, etc.)<sup>6–11</sup> countermeasures. These methods are effective under certain conditions, but each of them has limitations, such as water conservancy needs a lot of manpower, phytoremediation takes much time and tends to be

restricted by climate conditions, and chemical methods have high costs. Meanwhile, these methods are aimed to remediate all the SS in a field, so they have rather long time periods, high cost, and low efficiency. Hence, they have difficulty meeting the demands of the current agriculture development in a SS area. Fundamentally, soil salinization and alkalization are mainly attributed to the issues of water and salt.<sup>12</sup> Therefore, it is required that an effective approach to control the migration of water and salt in SS is developed. It may be more effective and of lower cost to just focus on the microenvironment (microregion) around the roots of crops in SS. Consequently, we are trying to develop an approach to remediate the microenvironment of SS.

In this article, a facile and promising approach to remediate the microenvironment of SS is provided using a novel fertilizer named saline–alkali soil remediating fertilizer (SSRF). SSRF was obtained by adding a saline–alkali soil remediating agent (SSRA), a complex of attapulgite (ATP), phosphogypsum (PG), sodium polyacrylate (SP), and weathered coal (WC), to

**Received:** December 4, 2014

**Revised:** January 4, 2015

**Published:** January 12, 2015

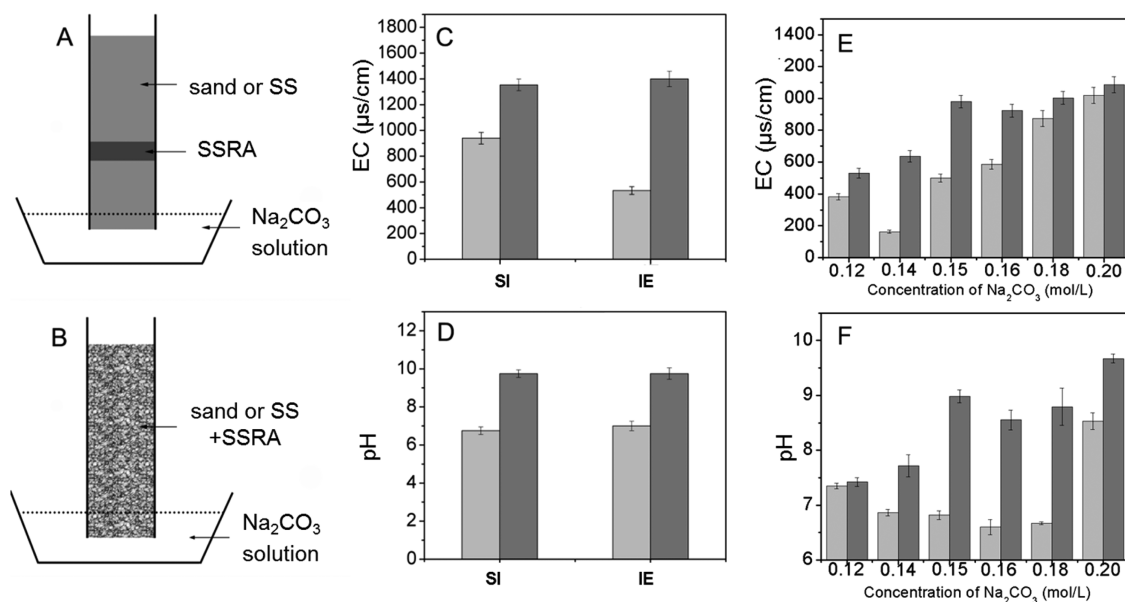


**Figure 1.** (A, B) Schematic diagrams of SI and IE systems. (C, D) Remediation effects of SSRA (1 g) on the salinity and alkalinity of sand (light gray, with SSRA; dark gray, without SSRA). (E, F) Remediation effects of SSRA (1 g) on the salinity and alkalinity of SS in SI system (light gray, with SSRA; dark gray, without SSRA).

traditional fertilizer (TF). Therein the following could occur: ATP could effectively retain fertilizer nutrients in soil. SP could possess a high retaining capacity on water. PG could significantly reduce the salinity and alkalinity in SS through ion exchange and deactivation. WC could reduce the salinity and alkalinity through acid–base neutralization. Also, SSRF could form three-dimensional micro/nanonetworks in SS and possess high abilities on water and nutrient retaining, ion exchange, and pH adjusting; thus, it could effectively remediate the microenvironment of SS.

## MATERIALS AND METHODS

**Material.** The original attapulgite powder (100–200 mesh) was provided by Mingmei Co., Ltd. (Anhui, China). Phosphogypsum (PG) was provided by Anhui Hongsifang Co., Ltd. (Anhui, China). Weathered coal (WC) was provided by Pingxiang Huli Weathered Coal Co. (Jiangxi, China). Other chemicals, analytical reagent grade without any purification, were purchased from Sinopharm Chemical Reagent Co. (Shanghai, China). Deionized water was used throughout this work except the pot experiments. Corn seeds were provided by DuPont Pioneer Co. (Liaoning, China). The SS sample with pH of 9.0 and salinity of 0.7% was taken from Pingluo county in Ningxia Province of China.

**Preparation of SSRF.** ATP, PG, SP, and WC with different weight ratios were mixed together to obtain several complexes, and their effects on the salinity and alkalinity of sand were investigated in order to find the optimal one that was designated as SSRA. Afterward, a designated amount of SSRA was added to urea (U) or NH<sub>4</sub>Cl (N) to obtain SSRU or SSRN, respectively, as the model SSRF.

**Remediation Performance on Salinity and Alkalinity.** The remediation performance of SSRA was investigated in salt insulation (SI) and ion exchange (IE) experiment systems. As for the SI system, 15 g of dry sand (or SS) was placed into a centrifuge tube (50 mL) with a hole (diameter of 2 mm) at the bottom. Then 1 g of SSRA was placed on the top of sand (or SS), and 40 g of sand (or SS) was placed on the top of the sample with a piece of filter paper between the top sand (or SS) layer and the SSRA layer. Afterward, the bottom of the resulting centrifuge tube was soaked in a beaker with 30 mL of Na<sub>2</sub>CO<sub>3</sub> solution (0.1 mol/L for the sand column and different concentrations for the SS column) as the simulated saline–alkali solution. After 12 h, the top sand (or SS) layer was transferred to 100

mL of deionized water to obtain a suspension, and the resulting suspension was stirred (100 rpm) for 30 min. After centrifugation (12000 rpm) for 5 min, the pH and electrical conductivity (EC) of the supernatant were measured. As for the IE system, 40 g of dry sand (or SS) was well mixed with 1 g of SSRA, and then the mixture was placed into a centrifuge tube (50 mL) with a hole (diameter of 2 mm) at the bottom. After that, the bottom of the resulting centrifuge tube was soaked in a beaker with 30 mL of Na<sub>2</sub>CO<sub>3</sub> solution (0.1 mol/L for the sand column and different concentrations for the SS column) as the simulated saline–alkali solution. After 4 h, the resulting mixture was transferred from the tube to 100 mL of deionized water to obtain a suspension, and the suspension was stirred (100 rpm) for 30 min. After a centrifugation (12,000 rpm) for 5 min, the pH and EC of the supernatant were measured. Meanwhile, the control experiments without SSRA were carried out in dry sand (or SS).

**Leaching Behavior Investigation.** Thirty grams of dry sand (or SS) (150–200 mesh) was put into a centrifuge tube (50 mL) with a hole (diameter of 2 mm) at the bottom. Then 5 mL of deionized water was added to keep the humidity of sand (or SS). Sample (1 g of SSRU or SSRN) was buried (cylinder shape, diameter of 2.0 cm, and depth of 1 cm) in the sand (or SS) (humidity of 30%) at 30 °C and covered with another 15 g of dry sand (or SS). A total of 50 mL of deionized water was sprayed over the top of the sand (or SS) layer to collect the leachate, in which the concentration of urea (or NH<sub>4</sub>Cl) was measured afterward.<sup>13–15</sup> Meanwhile, the control experiment was carried out using TF (urea or NH<sub>4</sub>Cl) with the same nutrient as SSRU or SSRN. The leaching loss control ratio (LLCR) was calculated through the following equation: LLCR = [(leaching loss amount of TF – leaching loss amount of SSRF)/leaching loss amount of TF] × 100%.

**Migrate-to-Surface (MS) Performance.** First, 20 g of dry sand (or SS) was placed into a plastic cup, and 10 mL of deionized water was slowly sprayed to the sand (or SS). Then, 2 g of SSRU or SSRN was spread on the sand (or SS), and 20 g of dry sand (or SS) was placed evenly on the top. Subsequently, 10 mL of Na<sub>2</sub>CO<sub>3</sub> solution (0.1 mol/L for the sand column and 0.15 mol/L for the SS column) was slowly added into the sand (or SS) column. Afterward, the system was placed at 35 °C for 12 h, and then, a layer of top sand (or SS) (1 cm depth) of the resulting system was transferred into 50 mL of deionized water. The resulting suspension was stirred (100 rpm) for 30 min. After a centrifugation (12,000 rpm) for 5 min, the concentration of urea (or NH<sub>4</sub>Cl) in the supernatant was measured to get the MS amount of urea (or NH<sub>4</sub>Cl). Meanwhile, the control

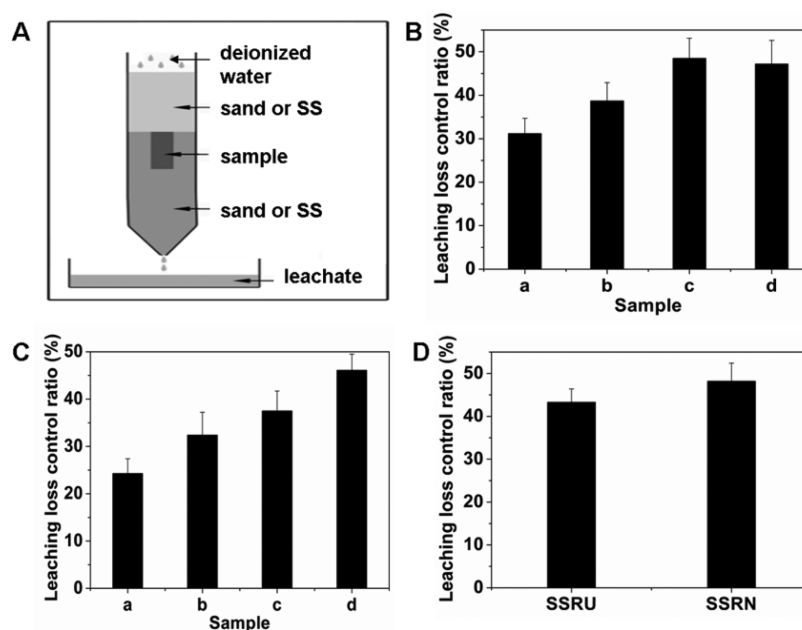


**Figure 2.** (A) Schematic diagram of leaching system. (B, C) Leaching loss control performance of SSRU and SSRN with different  $W_F/W_{SSRA}$  ratios of 9:0.6 (a), 9:0.8 (b), 9:1 (c), and 9:1.2 (d) in sand. (D) Leaching loss control performance of SSRU ( $W_U/W_{SSRA} = 9:1$ ) and SSRN ( $W_N/W_{SSRA} = 9:1.2$ ) in SS.

experiment was carried out using TF (urea (or  $\text{NH}_4\text{Cl}$ ) with the same nutrient as SSRU (or SSRN)) instead of SSRF. The MS loss control ratio (MLCR) of SSRF was calculated through the following equation:  $\text{MLCR} = [(\text{MS amount of TF} - \text{MS amount of SSRF}) / \text{MS amount of TF}] \times 100\%$ .

**Pot Experiment.** A designated amount of SSRF or SSRA was mixed with 20 g of soil to get a mixture which was then buried (cylinder shape) between two soil layers (800 g in the top layer and 150 g in the bottom layer) in a PVC tube (cylinder shape, diameter of 7.5 cm, and height of 25 cm) with the bottom covered by a nylon net. Two corn seeds were planted in the top layer (10 cm deep), and the tube stood in a dish. A total of 40 mL of  $\text{Na}_2\text{CO}_3$  solution (0.15 mol/L) was added to the dish every day. The system was kept in a greenhouse at 20 °C, and the growth of the corn was observed in order to investigate the remediation effect of SSRA or SSRF on SS.

**Field Test.** Field tests of corn (24,000 seeds per acre) were carried out in two neighboring fields (0.5 acre and 5 acres) (pH of 9.0 and salinity of 0.7%) in Ningxia Province of China. A designated amount of SSRU was spread evenly onto the soil surface before ploughing on April 25. The influence of SSRU with designated amount on the germination rate, stem diameter, height, and yield of corn, and length and diameter of corncob was investigated on September 10 in a mature period. The increasing ratio of SSRF to TF on these characteristics of corn was calculated through the following equation:  $\text{increasing ratio} = [(\text{measured result of the corn with SSRF} - \text{measured result of the corn with TF}) / \text{measured result of the corn with TF}] \times 100\%$ .

**Characterization.** The morphology was observed on a scanning electron microscope (SEM) (Sirion 200, FEI Co., U.S.A.). The structure and interaction analyses were performed using a TTR-III X-ray diffractometer (XRD) (Rigaku Co., Japan) and a Fourier transform infrared (FTIR) spectrometer (iS10, Nicolet Co., U.S.A.). The concentration of urea (or  $\text{NH}_4\text{Cl}$ ) was measured using an ultraviolet–visible (UV–vis) spectrophotometer (UV2550, Shimadzu Co., Japan). The concentration of  $\text{Na}^+$  or  $\text{Ca}^{2+}$  was measured using an inductively coupled plasma–optical emission spectrometer (ICP-OES) (Optima 7300 DV, PerkinElmer Co., U.S.A.). The electrical conductivity was detected by a conductivity meter (DDS-307, Shanghai Yidian Scientific Instrument Co., Ltd, China). The pH was detected by a pH meter (FE-20k, Mettler-Toledo Instrument Co., Ltd., Switzerland).

## RESULTS AND DISCUSSION

**Remediation Effect on Salinity and Alkalinity.** The remediation effects of different mixing ratios of ATP, PG, SP, and WC on the salinity and alkalinity of sand were investigated through SI and IE experiments (Figures S1 and S2, Supporting Information), and the optimal effect was obtained under the ratio of  $W_{\text{ATP}}:W_{\text{PG}}:W_{\text{SP}}:W_{\text{WC}} = 60:30:1:12$ ; therefore, this ratio was selected for the formation of SSRA. As shown in Figure 1, both in SI and IE systems (Figure 1A and B), SSRA exhibited significant effects on decreasing the salinity and alkalinity of sand (Figure 1C and D). As for SS, SSRA could show the obvious remediation effects on both salinity and alkalinity of SS treated with different concentrations of  $\text{Na}_2\text{CO}_3$ , especially between 0.14 and 0.16 mol/L (Figure 1E and F). Clearly, SSRA played a key role and could have the potential to be used in the remediation of SS.

**Fertilizer Nutrient Loss Control Behavior Investigation.** The loss control capacity of SSRA on fertilizer in sand (or SS) was also investigated (Figure 2A). Herein, SSRA was added to TF to obtain SSRF. As shown in Figure 2B and C, SSRA could reduce the leaching loss amounts of U and N in sand, and LLCR increased with the increasing weight ratios of SSRA, reaching the highest value at  $W_U/W_{SSRA} = 9:1$  and  $W_N/W_{SSRA} = 9:1.2$ . Therefore, the optimal  $W_U/W_{SSRA}$  for controlling the leaching loss of U was 9:1, and the optimal  $W_N/W_{SSRA}$  was 9:1.2. The results in SS (Figure 2D) indicated that, under the optimal conditions, SSRA could efficiently control the loss of fertilizer nutrients through leaching so that sufficient nutrients were retained in the top layer of soil, which was beneficial for increasing the utilization efficiency and lowering the pollution risk of fertilizer.

Fertilizer nutrients could discharge to environment through not only leaching but also runoff and volatilization. Generally, TF in soil tended to migrate to the soil surface with water through evaporation, and then, the nutrients on the soil surface were transferred to the environment more easily through runoff and volatilization. Therefore, it was important to prevent the



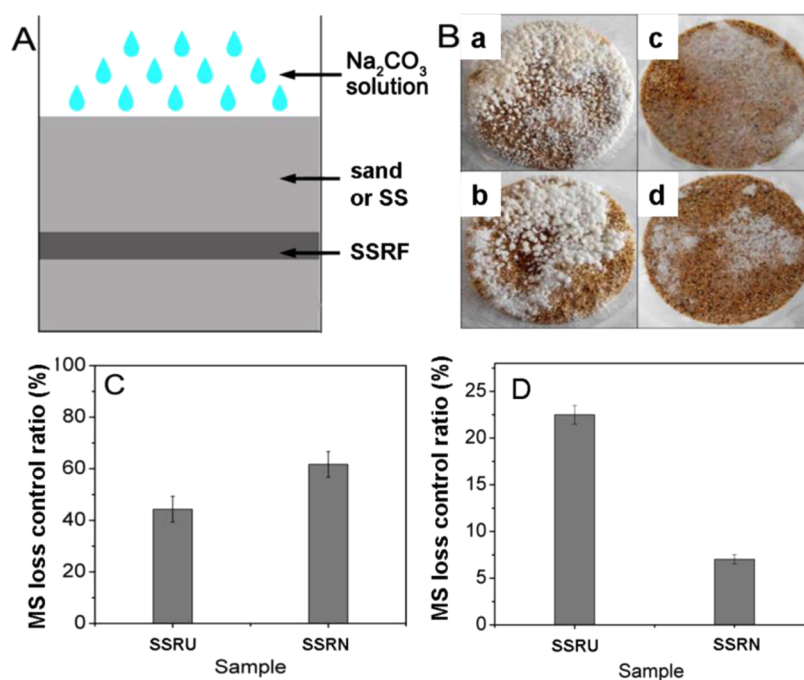


**Figure 3.** (A) Schematic diagram of the MS experiment system. (B) Digital photographs of the experiment systems with U (a), SSRU (b), N (c), and SSRN (d) in sand after MS process. (C, D) MS loss control rates of SSRF in sand and SS.

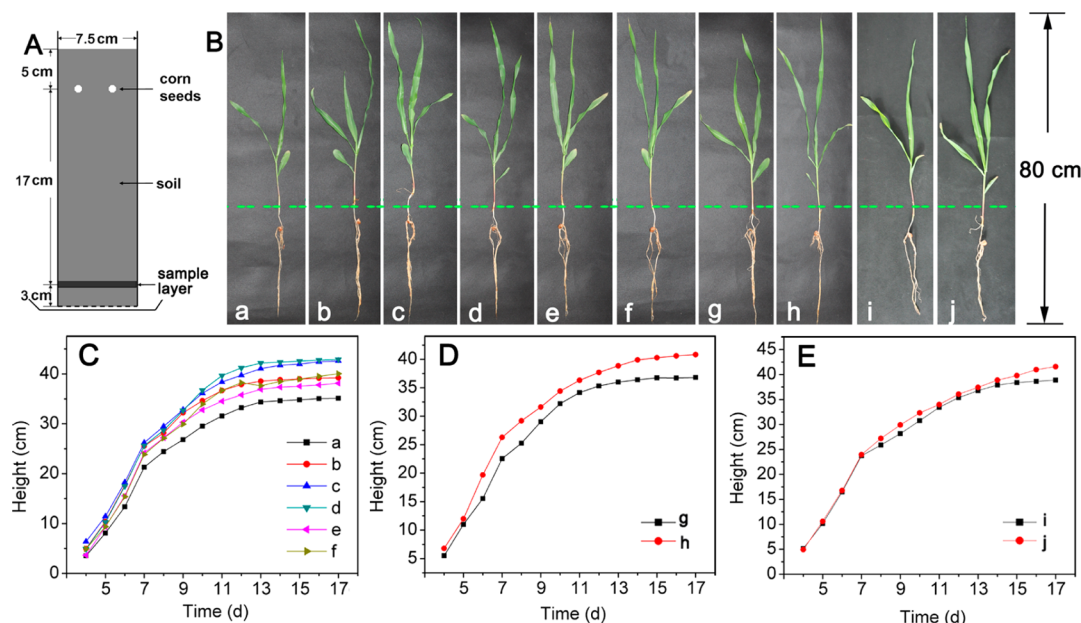


**Figure 4.** (A) Schematic diagram of the pot experiment system (sample layer: 20 g soil mixed with different samples). (B) Digital photographs of the corn seedlings growing in soil with different samples: (a) blank, (b) SSRA (0.2 g), (c) SSRA (0.4 g), (d) SSRA (0.6 g), (e) SSRA (0.8 g), (f) SSRA (1.0 g), (g) U (0.2 g), (h) SSRU (0.2 g of U + 0.022 g of SSRA), (i) N (0.2 g), and (j) SSRN (0.2 g of N + 0.027 g of SSRA). (C, D) Influences of SSRA, SSRU, and SSRN on the height of corn.

fertilizer nutrients from migrating to the soil surface in order to reduce the loss of nutrients. It is shown clearly from Figure 3 that SSRU and SSRN exhibited obvious MS loss control abilities in sand and SS. That was to say, SSRA could significantly reduce the MS loss amounts of fertilizer, and thus, more nutrients could be retained in the soil, contributing to a higher fertilizer utilization.

**Effects of SSRA or SSRF on Corn in SS.** On the basis of the preceding analysis, SSRA showed high performance on reducing the salinity and alkalinity of SS and controlling the

loss of fertilizer nutrients. Hence, SSRA could potentially promote the growth of crops in SS. As shown in Figure 4B and C, the pot experiment indicates that SSRA could promote the growth of the root and height of corn at seedling stage. The height of the corn seedling increased with the SSRA amounts from 0.2 to 0.6 g and then decreased (>0.6 g), achieving the optimal SSRA amount of 0.6 g in 20 g soil. Meanwhile, SSRU and SSRN also displayed promotion effects on the growth of corn in seedling stage (Figure 4B, D, and E). These results indicated that SSRA, alone or together with TF, could be used

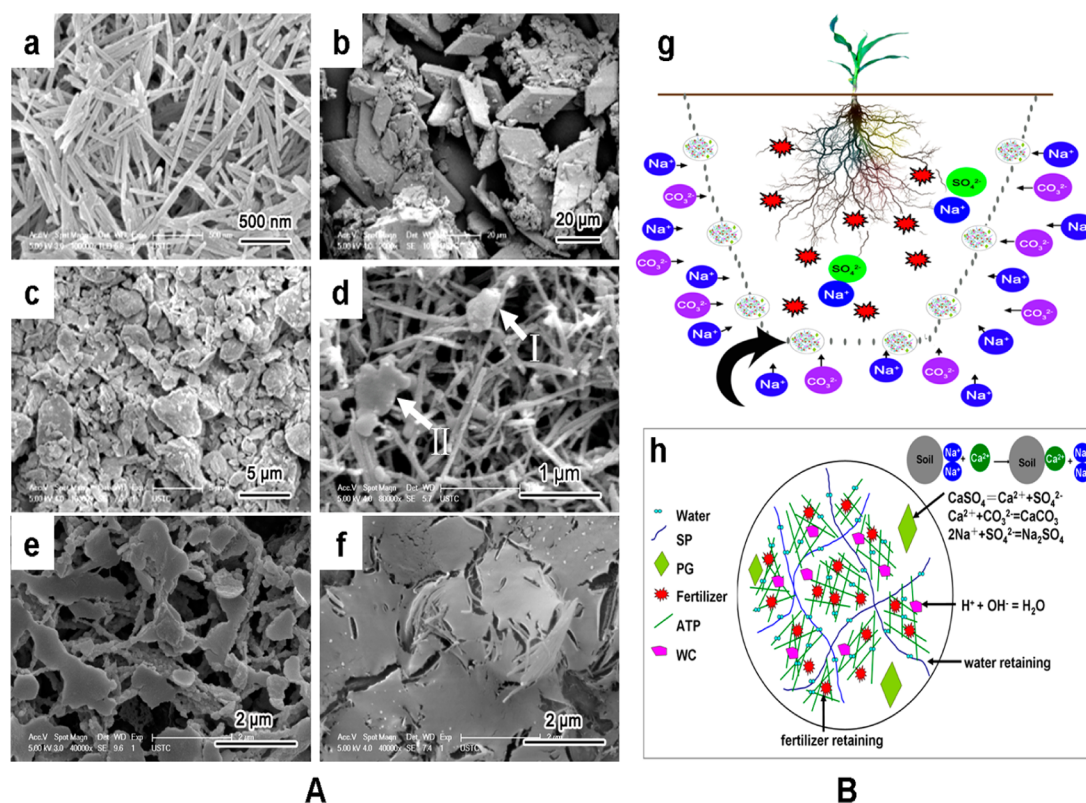


**Figure 5.** (A) SEM images of ATP (a), PG (b), WC (c), SSRA (d), SSRU (e), and SSRN (f). (B) Schematic diagrams of the mechanism (g) and microstructure (h) of SSRF.

as an effective remediation agent for SS to facilitate the growth of crop in SS. In addition, SSRF could also promote the growth of corn in regular soil (Figure S3, Supporting Information), which was probably because of the retaining ability of SSRF on water and nutrients.

**Field Test.** Besides the pot experiment, the field tests of SSRF on corn in SS were performed. Figure S4A and B of the Supporting Information illustrated that SSRU with equal or 90% nutrients of TF could notably promote the germination rate, stem diameter, height, and yield of corn, and length and diameter of corncob in the field (0.5 acre) compared with TF. As for the field of 5 acres, SSRU also displayed a similar promotion effect on the corn compared with TF (with the equal nutrients). These results showed that SSRU could significantly improve the growth of corn in SS, which was probably resulted from the remediation effect of SSRU in SS.

**Mechanism Study.** Attapulgite  $[(Mg,Al)_4(Si)_8(O,OH,H_2O)_{26} \cdot nH_2O]$  is an important nanoclay formed by naturally aggregated nanorods approximately 800–2000 nm in length and 30–40 nm in width (Figure 5a).<sup>16–19</sup> This nanorods structure makes ATP have a large specific surface area and high adsorption capacity.<sup>20,21</sup> Moreover, there are many nanochannels in each ATP rod along the direction of the rod's axis, and plenty of  $-OH$  and  $-OH_2$  exist on the inner surface of the nanochannels and the rods surface.<sup>22</sup> Therefore, ATP tended to form hydrogen bonds (H-bonds) with SP, PG, and WC, and these H-bonds could probably induce ATP-SP-PG-WC (actually SSRA) to form three-dimensional micro/nanonetworks with ATP rods as the skeleton (Figure 5d). Compared with the aggregated ATP, the ATP skeleton possessed higher dispersion, more active chemical groups, larger specific surface area, and thus higher retaining ability on

fertilizer nutrients, which could be held in the networks of ATP-SP-PG-WC (Figure 5e and f). In addition, the formation of the ATP-SP-PG-WC networks made the dispersion of the PG (arrow I, Figure 5d) and WC (arrow II, Figure 5d) improved (Figure 5b–d), which was favorable for their effects of PG and WC on SS. PG could reduce the salinity and alkalinity in SS through ion exchange and deactivation ( $CaSO_4 = Ca^{2+} + SO_4^{2-}$ ;  $Ca^{2+} + CO_3^{2-} = CaCO_3$ ;  $2Na^+ + SO_4^{2-} = Na_2SO_4$ ) (Figure S5, Supporting Information), and WC with humic acid as the main ingredient could reduce the salinity and alkalinity through acid–base neutralization ( $H^+ + OH^- = H_2O$ ) (Figure 5h). As for SP, it displayed a high retaining capacity on water and fertilizer nutrients due to plenty of  $-COO-$  groups on the molecules. Furthermore, the formation of the ATP-SP-PG-WC networks facilitated the molecular chains of SP to contact more water and fertilizer molecules, which was helpful for the retaining capacity of SP on water and fertilizer.

On the basis of the preceding analysis, ATP-SP-PG-WC could form three-dimensional micro/nanonetworks, which exhibited good performance for retaining water and fertilizer through H-bonds (Figures 2 and 3) and reducing salinity/alkalinity through ion exchange, deactivation, and acid–base neutralization (Figure 1). Consequently, SSRF could establish a protecting area and remediate the SS microenvironment around the root of corn (Figure 5g), prevent the salts of SS such as  $Na^+$  and  $CO_3^{2-}$  from entering, and retain water and fertilizer in the microenvironment. That was to say, SSRF could significantly improve the microenvironment of SS and thus increase the saline–alkaline tolerance and facilitate the growth of corn (Figure S4, Supporting Information).

To further investigate the mechanism of SSRF, FTIR measurements on SSRA, SSRU and SSRN systems were performed. As shown in Figure 6A, SSRA possessed character-

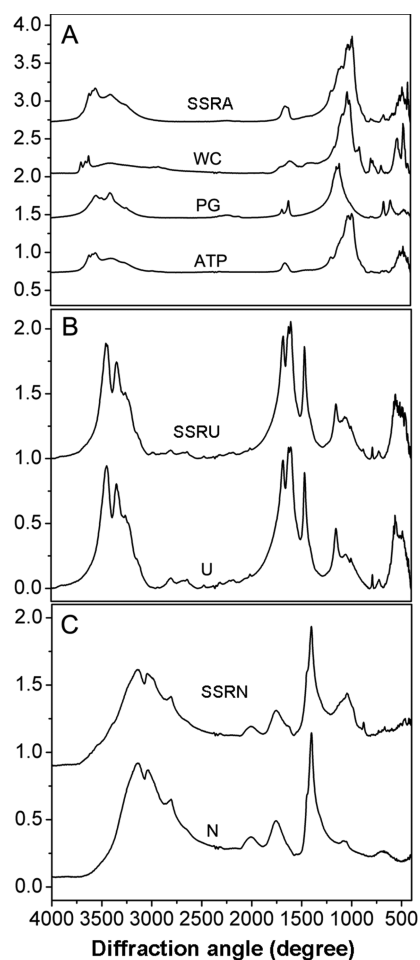


**Figure 6.** FTIR spectra of SSRA (A), SSRU (B), and SSRN (C) systems.

istic peaks of ATP ( $988\text{ cm}^{-1}$  for Si–O–Si stretching vibration), WC ( $1034\text{ cm}^{-1}$  for C=O bending vibration), and PG ( $3650\text{--}3950\text{ cm}^{-1}$  for –OH stretching vibration), indicating that these three components were well combined and existed in SSRA. Furthermore, the comparative strength of the peaks ( $488\text{ cm}^{-1}$  for the translation and  $509\text{ cm}^{-1}$  for the stretching vibration of –OH;  $988$  and  $1018\text{ cm}^{-1}$  for the stretching vibration of Si–O–Si;  $3551\text{ cm}^{-1}$  for –OH<sub>2</sub> stretching vibration;  $1034\text{ cm}^{-1}$  for C=O bending vibration;  $3650\text{--}3950\text{ cm}^{-1}$  for –OH stretching vibration) in SSRA were different compared with ATP, PG, or WC. This was probably because of the formation of hydrogen bonds among ATP (–OH and Si–O–Si), SP (–COO–), WC (C=O), and PG (–OH), which could contribute to the formation of ATP-SP-PG-WC networks. In addition, no obvious new peaks or peak shifts were found in SSRA compared with ATP, WC, and PG, indicating that no obvious chemical reaction occurred in the fabrication process of SSRA. In other words, the fabrication of SSRA was mainly a physical process.

It is shown in Figure 6B and C that the main characteristic peaks of SSRA ( $988$  and  $1018\text{ cm}^{-1}$  for Si–O–Si stretching vibration,  $3551\text{ cm}^{-1}$  for –OH<sub>2</sub> stretching vibration) and U ( $3447\text{ cm}^{-1}$  for –NH<sub>2</sub>,  $1721\text{ cm}^{-1}$  for C=O and  $1466\text{ cm}^{-1}$  for

C–N stretching vibration) or N ( $3140$  and  $3038\text{ cm}^{-1}$  for –NH stretching vibration, and  $1400\text{ cm}^{-1}$  for –NH bending vibration) could be found in the spectrum of SSRU or SSRN, suggesting that SSRA successfully bound to fertilizer. Furthermore, the comparative strength of the peaks in SSRU ( $1466\text{ cm}^{-1}$  for C–N stretching vibration) or SSRN ( $3140$  and  $3038\text{ cm}^{-1}$  for –NH stretching vibration, and  $1400\text{ cm}^{-1}$  for –NH bending vibration) were different compared with U or N, which was probably attributed to the formation of hydrogen bonds among SSRA (–OH and Si–O–Si), and U (C–N) or N (–NH). Additionally, new peaks or peak shifts were not found in SSRU or SSRN compared with U or N, illustrating that the formation of SSRU or SSRN was mainly a physical process.

Besides the FTIR, the X-ray diffraction measurements were carried out to obtain the crystal structure information on SSRA, SSRU, and SSRN. As shown in Figure S6A of the Supporting Information, the characteristic peaks of ATP ( $8.4^\circ$ ) (inset, Figure S6A, Supporting Information), PG ( $11.62^\circ$ ,  $23.36^\circ$ ,  $29.1^\circ$ ,  $31.08^\circ$ ), SP ( $7.86^\circ$ ), and WC ( $20.86^\circ$ ,  $26.62^\circ$ ) were all found in SSRA, indicating that ATP, PG, and WC were well combined. Meanwhile, no obvious new peaks or peak shift was found, presenting that no new substance was generated and no obvious chemical reaction occurred among ATP, PG, and WC. Additionally, the characteristic peaks of SSRA ( $11.62^\circ$ ) (insets, Figure S6B and C, Supporting Information), U ( $22.3^\circ$ ,  $24.64^\circ$ ,  $29.32^\circ$ ,  $31.68^\circ$ ,  $35.5^\circ$ ,  $37.1^\circ$ ,  $49.56^\circ$ ), or N ( $22.98^\circ$ ,  $32.68^\circ$ ,  $40.32^\circ$ ,  $46.86^\circ$ ,  $52.78^\circ$ ,  $58.28^\circ$ ,  $68.38^\circ$ ) could be found in SSRU or SSRN, as shown in Figure S6B and C, Supporting Information. These results illustrated that SSRA well bound to U or N. Moreover, those peaks ( $35.5^\circ$ ,  $37.1^\circ$ ) in SSRU were weakened compared with U alone, which was probably attributed to the lower crystallization of urea in some directions after addition of SSRA in aqueous phase. Also, compared with N alone, the peaks at  $22.98^\circ$ ,  $40.32^\circ$ ,  $58.28^\circ$  in SSRN were weakened, which was probably because of the lower crystallization of NH<sub>4</sub>Cl in these directions after binding with SSRA in aqueous phase.

## CONCLUSION

In summary, this work provides a high-performance fertilizer (SSRF) for remediating the microenvironment of SS. SSRF could effectively reduce the salinity and alkalinity in SS through ion exchange and pH adjusting. Meanwhile, SSRF could self-assemble to form three-dimensional micro/nanonetworks and thus display high retaining capacity on water and fertilizer nutrients. As a result, the improvement of the SS microenvironment, when using SSRF, could significantly facilitate the growth of crops and increase the saline–alkaline tolerance of crops.

## ASSOCIATED CONTENT

### Supporting Information

Figures S1 and S2 display the optimal ratio for ATP-PG-SP-WC to control salinity and alkalinity. Figure S3 shows the effects of SSRU and SSRN on the growth of corn in regular soil. Figure S4 shows the field test effect of SSRU in Ningxia Province of China. Figure S5 displays the effect of SSRA on the Na<sup>+</sup> and Ca<sup>2+</sup> concentrations in the SI and IE systems. Figure S6 is the result of XRD analysis. This material is available free of charge via the Internet at <http://pubs.acs.org>.



## AUTHOR INFORMATION

## Corresponding Authors

\*Tel.: +86-551-65786907. E-mail: swhx12@ahau.edu.cn (H.W.).

\*Tel.: +86-551-65786021. E-mail: xinzhang@ahau.edu.cn (X.Z.).

\*Tel.: +86-551-65595012. Fax: +86-551-65591413. E-mail: zyw@ipp.ac.cn (Z.W.).

## Notes

The authors declare no competing financial interest.

N.J. and D.C. are co-first authors.

## ACKNOWLEDGMENTS

The authors acknowledge financial support from the National Natural Science Foundation of China (21072002 and 21407151), Key Program of Chinese Academy of Sciences (KSZD-EW-Z-022-05), Science, Technology and Service Project of Chinese Academy of Sciences (KFJ-EW-STS-067), Scientific and Technological Project of Anhui Province of China (1206c0805014), and Comprehensive Agricultural Development Project of Ningxia Province of China (NTKJ-2014-07-02).

## REFERENCES

(1) Masoud, A. A.; Koike, K. Arid land salinization detected by remotely-sensed landcover changes: A case study in the Siwa region, NW Egypt. *J. Arid. Environ.* **2006**, *66*, 151–167.

(2) Sharma, B. R.; Minhas, P. S. Strategies for managing saline/alkali waters for sustainable agricultural production in South Asia. *Agric. Water Manage.* **2005**, *78*, 136–151.

(3) Saxena, N. P.; Saxena, M. C.; Ruckebauer, P.; Rana, R. S.; El-Fouly, M. M.; Shabana, R. Screening techniques and sources of tolerance to salinity and mineral nutrient imbalances in cool season food legumes. *Euphytica* **1994**, *73*, 85–93.

(4) Susarla, S.; Medina, V. F.; McCutcheon, S. C. Phytoremediation: An ecological solution to organic chemical contamination. *Ecol. Eng.* **2002**, *18*, 647–658.

(5) Han, L. P.; Liu, H. T.; Yu, S. H.; Wang, W. H.; Liu, J. T. Potential application of oat for phytoremediation of salt ions in coastal saline-alkali soil. *Ecol. Eng.* **2013**, *61*, 274–281.

(6) Suhayda, C. G.; Yin, L. J.; Redmann, R. E.; Li, J. D. Gypsum amendment improves native grass establishment on saline-alkali soils in northeast China. *Soil Use Manage.* **1997**, *13*, 43–47.

(7) Gharaibeh, M. A.; Eltaif, N. I.; Shunnar, O. F. Leaching and reclamation of calcareous saline-sodic soil by moderately saline and moderate-SAR water using gypsum and calcium chloride. *J. Plant Nutr. Soil Sci.* **2009**, *172*, 713–719.

(8) Guo, M. Y.; Liu, M. Z.; Liang, R.; Niu, A. Z. Granular urea-formaldehyde slow-release fertilizer with superabsorbent and moisture preservation. *J. Appl. Polym. Sci.* **2006**, *99*, 3230–3235.

(9) Qi, C. X. Chinese Patent CN 102443401, 2014, , pp B16–B30.

(10) Zhang, H. W. Chinese Patent, CN 102352257, 2012, pp A7–A28.

(11) Wu, Y. P.; Li, Y. F.; Zheng, C. Y.; Zhang, Y. F.; Sun, Z. J. Organic amendment application influence soil organism abundance in saline. *Eur. J. Soil Biol.* **2013**, *54*, 32–40.

(12) Chhabra, R. Classification of salt-affected soils. *Arid Land Res. Manage.* **2004**, *19*, 61–79.

(13) Knorst, M. T.; Neubert, R.; Wohlrab, W. Analytical methods for measuring urea in pharmaceutical formulations. *J. Pharm. Biomed. Anal.* **1997**, *15*, 1627–1632.

(14) Hussain, I.; Mahmood, Z.; Yasmeen, R.; Jahangir, M.; Hammed, R.; Nasir, R. Assay of urea with p-dimethylaminobenzaldehyde. *J. Chem. Soc. Pakistan* **2002**, *24*, 122–128.

(15) Ivanov, V. M.; Figurovskaya, V. N.; Barbalat, Y. A.; Ershova, N. I. Chromaticity characteristics of  $\text{NH}_2\text{Hg}_2\text{I}_3$  and  $\text{I}_2$ : Molecular iodine

as a test form alternative to Nessler's reagent. *J. Anal. Chem.* **2005**, *60*, 629–632.

(16) Giustetto, R.; Xamena, F. X. L.; Ricchiardi, G.; Bordiga, S.; Damin, A.; Gobetto, R.; Chierotti, M. R. Maya blue: A computational and spectroscopic study. *J. Phys. Chem. B* **2005**, *109*, 19360–19368.

(17) Huang, J. H.; Liu, Y. F.; Jin, Q. Z.; Wang, X. G.; Yang, J. Adsorption studies of a water soluble dye, reactive red MF-3B, using sonication-surfactant-modified attapulgite clay. *J. Hazard. Mater.* **2007**, *143*, 541–548.

(18) Chen, H.; Wang, A. Q. Kinetic and isothermal studies of lead ion adsorption onto palygorskite clay. *J. Colloid Interface Sci.* **2007**, *307*, 309–316.

(19) Xue, S. Q.; Reinholdt, M.; Pinnavaia, T. J. Palygorskite as an epoxy polymer reinforcement agent. *Polymer* **2006**, *47*, 3344–3350.

(20) Chiari, G.; Giustetto, R.; Ricchiardi, G. Crystal structure refinement of palygorskite and Maya Blue from molecular modeling and powder synchrotron diffraction. *Eur. J. Miner.* **2003**, *15*, 21–33.

(21) Xiang, Y. B.; Wang, M.; Sun, X.; Cai, D. Q.; Wu, Z. Y. Controlling pesticide loss through nanonetworks. *ACS Sustainable Chem. Eng.* **2014**, *2*, 918–924.

(22) Galan, E. Properties and applications of palygorskite-sepiolite clays. *Clay Miner.* **1996**, *31*, 443–453.